Hyper-parallel tempering Monte Carlo simulations of Ar adsorption in new models of microporous non-graphitizing activated carbon: effect of microporosity

2007 J. Phys.: Condens. Matter 19 406208

(http://iopscience.iop.org/0953-8984/19/40/406208)

IOP PUBLISHING JOURNAL OF PHYSICS: CONDENSED MATTER

J. Phys.: Condens. Matter **19** (2007) 406208 (17pp) doi:10.1088/0953-8984/19/40/406208

Hyper-parallel tempering Monte Carlo simulations of Ar adsorption in new models of microporous non-graphitizing activated carbon: effect of microporosity

Artur P Terzyk[1,5,6], Sylwester Furmaniak[1], Piotr A Gauden[1], Peter J F Harris[2,5,7], Jerzy Włoch[3] and Piotr Kowalczyk[4]

[1] Department of Chemistry, Physicochemistry of Carbon Materials Research Group, N Copernicus University, Gagarin Street 7, 87-100 Toruń, Poland
[2] Centre for Advanced Microscopy, University of Reading, Whiteknights, Reading RG6 6AF, UK
[3] Department of Chemistry, Synthesis and Modification of Carbon Materials Research Group, N Copernicus University, Gagarin Street 7, 87-100 Toruń, Poland
[4] Division of Chemical Engineering, The University of Queensland, Brisbane, QLD 4072, Australia

E-mail: aterzyk@chem.uni.torun.pl and p.j.f.harris@rdg.ac.uk

Received 21 June 2007, in final form 18 July 2007
Published 11 September 2007
Online at stacks.iop.org/JPhysCM/19/406208

Abstract

The adsorption of gases on microporous carbons is still poorly understood, partly because the structure of these carbons is not well known. Here, a model of microporous carbons based on fullerene-like fragments is used as the basis for a theoretical study of Ar adsorption on carbon. First, a simulation box was constructed, containing a plausible arrangement of carbon fragments. Next, using a new Monte Carlo simulation algorithm, two types of carbon fragments were gradually placed into the initial structure to increase its microporosity. Thirty six different microporous carbon structures were generated in this way. Using the method proposed recently by Bhattacharya and Gubbins (BG), the micropore size distributions of the obtained carbon models and the average micropore diameters were calculated. For ten chosen structures, Ar adsorption isotherms (87 K) were simulated via the hyper-parallel tempering Monte Carlo simulation method. The isotherms obtained in this way were described by widely applied methods of microporous carbon characterisation, i.e. Nguyen and Do, Horvath–Kawazoe, high-resolution α_s plots, adsorption potential distributions and the Dubinin–Astakhov (DA) equation. From simulated isotherms described by the DA equation, the average micropore diameters were

[5] Authors to whom any correspondence should be addressed.
[6] http://www.chem.uni.torun.pl/~aterzyk/
[7] http://www.personal.rdg.ac.uk/~scsharip/pjfhhome.htm

calculated using empirical relationships proposed by different authors and they were compared with those from the BG method.

S Supplementary data are available from stacks.iop.org/JPhysCM/19/406208

(Some figures in this article are in colour only in the electronic version)

1. Introduction

Despite their importance in areas of technology such as catalysis and the purification of gas and water supplies, the detailed structure of activated carbons is still unknown [1, 2]. Recent studies applying the reverse Monte Carlo (RMC) technique [1, 3–7] have led to some very interesting results in this field, and the most important conclusion from this work is that the slit-like model of carbon pores is far from reality. Interesting and important are the results published recently by Coasne *et al* [8], showing that the filling pressure for an assembly of slit pores is much lower than that for disordered porous carbon. This puts into question the reality of the pore size distribution (PSD) curves obtained from adsorption measurements via typical adsorption apparatus connected with, for example, the density functional theory (DFT) software, where the local isotherms are simulated for ideal carbon slits. A notable feature of PSDs determined in this way is that they usually have two peaks, regardless of the origin of the carbon [9–13]. This problem was partially discussed by us recently [14–16].

In the current study we are concerned with modelling the porosity and adsorptive properties of microporous carbon. A model of activated carbon proposed a few years ago by Harris *et al* [2, 17–20] is the starting point for our considerations. These authors initiated a series of studies of typical non-graphitizing microporous carbons using high-resolution transmission electron microscopy (HRTEM) in the mid-1990s. By careful examination of both freshly prepared and heat-treated carbons, it was concluded that the structure consisted of discrete fragments of curved carbon sheets, in which pentagons and heptagons are dispersed randomly throughout networks of hexagons, as illustrated in figure 1 [17–20]. This fullerene-like model explains many properties of so-called 'hard' synthetic activated carbons, especially their microporosity and high resistance to graphitization. A number of other groups have also found evidence for fullerene-related structures in 'conventional' carbons [21–28]. The aim of this study is to compare the data obtained from molecular simulations on such structures (having different micropore size distributions) with those obtained from adsorption measurements. Knowing the geometric coordinates of atoms in the simulation box, as the reference method of the PSD calculation, we applied the method proposed recently by Bhattacharya and Gubbins [29]. They reported a new technique of fast computation of the PSD of model materials, from knowledge of the molecular coordinates. The PSD is defined as the statistical distribution of the radius of the largest sphere that can be fitted inside a pore of a given point. This method was successfully tested in our recent research for different ideal and defected carbon slit-like pores [16]. In the current study we assume that the initial model, proposed by Harris and colleagues, is very close to the true structure of microporous non-graphitizing carbons. Next, using the MC simulation program, 36 different microporous carbon models are created. The method of Bhattacharya and Gubbins is used to calculate the PSD curves, together with the average effective micropore diameters. For ten carbon structures obtained in such a way with gradually developing microporosities, Ar adsorption isotherms are simulated using the hyper-parallel tempering MC simulations proposed by Yan and de Pablo [30]. This method was developed to avoid the typical problems occurring in simulations of complex systems, i.e. the trapping

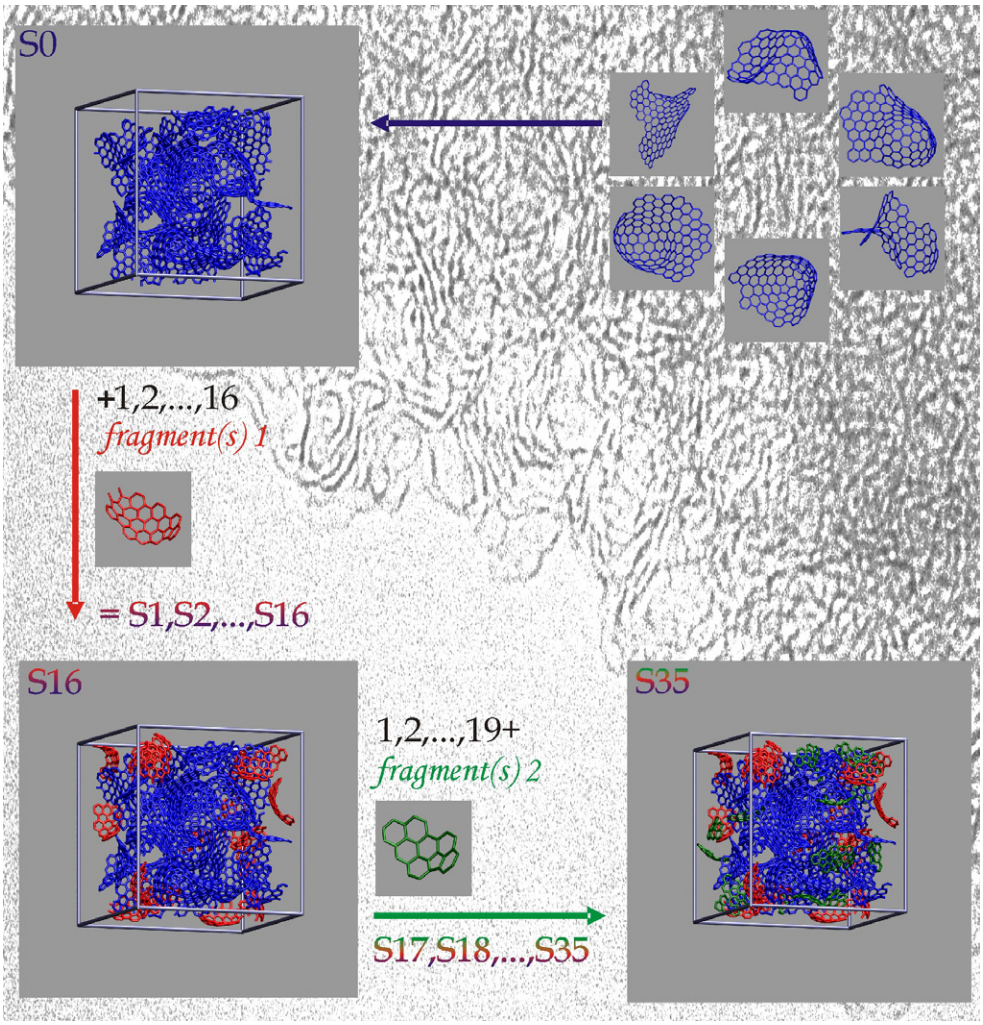

Figure 1. Illustration of the individual fragments forming the initial microporous structure S0, and the procedure for creating carbon structures from this by the addition (using the Monte Carlo algorithm) of fragments 1 and 2. Simulation boxes with structures S0, S16 and S35 are shown. The background shows a typical HRTEM picture of microporous 'hard' carbon.

of configurations in local energy minima precluding sampling of other, relevant regions of the phase space.

The simulated isotherms and the PSDs from the BG method are next used for testing the validity of the proposed models of hard carbons, and for checking the reliability of different approaches widely used for characterising the microporosity of activated carbons, namely: the HK and ND methods, high-resolution α_s plots, adsorption potential distributions (APD) and the Dubinin–Astakhov (DA) adsorption isotherm equation.

The simplest method for calculating the PSD of micropores applied in this study is the Horvath–Kawazoe (HK) condensation-approximation-type method [31, 32], with the parameters characteristic for the carbon–Ar system [33]. The next method is the one proposed by Nguyen and Do (ND) [9, 11, 34–40]. This relatively simple approach is faster than the non-

local density functional theory (NLDFT) and leads to exactly the same PSDs (as was shown for many porous materials having different structures and origin: see the results published by Kowalczyk and co-workers [12]). The basis of 82 ND local isotherms was generated in the current study for the same effective width range (from 0.465 to 233.9 nm), as local isotherms in the DFT software (DFT PLUS, ASAP 2010, Micromeritics). Additional details and values of the parameters for the ND [36, 41] model can be found elsewhere. Finally, the PSDs were calculated using the 'Karolina' algorithm (this algorithm is faster than the previously developed ASA [11, 34, 35]) to solve the unstable linear Fredholm integral equation of the first kind [42].

The applicability of the high-resolution α_s plot method for carbons was studied extensively by Setoyama *et al* [43]. They drew many interesting conclusions, confirming the mechanism of primary and secondary micropore filling in carbons having a slit-like system of pores. From GCMC simulation results they related the shape of these plots and the presence of so-called 'filling' and 'condensation' swings (FS and CS, respectively [44, 45]) to the PSD, adsorption mechanisms in slits, and their diameters. Summing up, for a system of carbon slits having a micropore width of around 0.5 nm the FS is observed on the α_s plot. For adsorbents having dispersed microporosity, the CS appears (here both swings occur) and, finally, the α_s plot is of CS type if micropores have diameters larger than about 1 nm. Therefore, it is interesting to check which type of α_s plots will be obtained from isotherms simulated on structures from this study, and to check the validity of conclusions obtained based on the assumption of a slit-like model of carbon porosity for the fullerene-like carbon structures. It should be mentioned here that the GCMC simulation studies of Biggs *et al* [46] performed on strongly heterogeneous carbon models questioned the primary and secondary micropore filling mechanism of Sing *et al* [44, 45]. Moreover, the authors concluded that the specifics of the small-α_s character cannot be attributed unambiguously to particular pore sizes, except in the simplest cases such as adsorption on slit pores of infinite extent and, even then, only when the surfaces of the reference and the porous solid are similar.

The next method that was tested (APD) also plays an important role in porosity characterisation, since it is modeless. By simple differentiation of the adsorption isotherm, one can associate the shape of the APD curve with the presence or absence of microporosity and with the adsorption mechanism. This concept was significantly developed by Jaroniec and co-workers [47], who related the maxima on APD curves to the DFT average slit-like pore diameters.

Finally, the theory of volume filling of micropores (TVFM) formulated by Dubinin *et al* [48–53] is tested as being a very simple and extremely popular approach. An enormous number of experimental adsorption systems have been described by this model; however, after the expansion of computer simulations, this approach was criticised intensively by a number of authors. This criticism centres on the fundamental assumption of the Dubinin–Astakhov (DA) concept, i.e. the idea that the DA equation describes adsorption in a homogeneous pore system (i.e. with a constant pore diameter). In other words, it was postulated, on the basis of much experimental data, that if DA works well, then the carbon can be described as having a relatively homogeneous micropore system. Following this assumption, many authors proposed relations between the average effective pore diameter (H_{eff}) and the parameters of the DA adsorption isotherm (they are collected in table 1).

Therefore, it will be interesting to compare the calculated effective pore diameters (obtained from the fitting of simulated isotherms by the DA equation and using E_0 versus H_{eff} relations) for the studied microporous structures with those predicted from the reference BG method. A related aim of this study is to test the validity of some conclusions presented in the paper by Chen and Yang [72]. They derived the DA adsorption equation based on statistical mechanics. In this important study the authors concluded that the parameter n of this equation

Table 1. Relationships between the characteristic energy of adsorption (E_0, [kJ mole^{-1}]) (equation (3)) and the average micropore diameter, (H_{eff}, [nm]).

Equation	Author	Reference	Abbreviation
$\frac{H_{\text{eff}}}{d_A} = \frac{a_{1(\text{all})}}{1+b_{1(\text{all})}\times\exp[-c_{1(\text{all})}\times n]} + \frac{a_{2(\text{all})}+b_{2(\text{all})}\times n+c_{2(\text{all})}\times n^2}{E_0}$	Terzyk *et al*	[54–59]	T1
$\frac{H_{\text{eff}}}{d_A} = \left(\frac{a_{1(\text{mic})}\times n}{b_{1(\text{mic})}+n}\right)\times\left(\frac{a_{2(\text{mic})}\times n}{b_{2(\text{mic})}+n}\right)^{E_0}\times E_0^{\left(\frac{a_{3(\text{mic})}\times n}{b_{3(\text{mic})}+n}\right)}$	Terzyk *et al*	[55–58, 60–62]	T2
$H_{\text{eff}} = \frac{16.5}{E_0}$			St1
$H_{\text{eff}} = \frac{18}{E_0}$	Stoeckli *et al*	[63–68]	St2
$H_{\text{eff}} = \left(\frac{30}{E_0}\right) + \left(\frac{5705}{E_0^3}\right) + 0.028\cdot E_0 - 1.49$			St3
$H_{\text{eff}} = 6.6 - 1.79\ln(E_0)$	McEnaney	[69, 70]	McE1
$H_{\text{eff}} = 4.691\exp[-0.0666E_0]$			McE2
$H_{\text{eff}} = \left(\frac{10.416}{E_0}\right) + \left(\frac{13.404}{E_0^3}\right) + 0.008212E_0 + 0.5114$	Jaroniec and Choma	[71]	JCh

is the structural parameter, i.e. for a given adsorbate the larger the value of n, the higher the value of the potential energy of adsorbed molecules in the force field of the adsorbent. A consequence of this is the occurrence of general relationships between the parameter E_0 of the DA model and the potential energy, leading to the inverse relationships between H_{eff} and E_0. This problem was also discussed previously by other authors [15].

2. Calculation details

2.1. Creating microporous carbon structures using the Monte Carlo (MC) algorithm

The initial microporous structure, named S0, is shown in figure 1. Using the MC program, a fragment containing 52 carbon atoms (*fragment 1*), also shown in figure 1, was placed randomly in structure S0 (see supplementary data available at stacks.iop.org/JPhysCM/19/406208). First, the position of the centre of mass of the fragment was sampled; next, the code samples the angular orientation. The fragment is accepted in the structure if an overlap does not occur, i.e. if the distance between pairs of carbon atoms (between fragment and structure) is larger than 0.17 nm. The configurations of each structure were recorded by the program after the addition of each fragment. It was possible to add 16 fragments to S0 (the obtained structures are labelled from S1 to S16). Next, 19 carbon structures were obtained from structure S16 using the same method but using a fragment approximately half the size (*fragment 2*, containing 27 carbon atoms; figure 1). The 19 structures obtained in this way were labelled from S17 to S35. Figure 1 shows the method used for the creation of carbon structures: S0—S35. It should be noted that all animations and graphics collected in figures 1 and 4 were created using the VMD program [73].

2.2. Density of carbon structures

The density of the carbon structures was determined in the following way. The volume was calculated on the basis of Monte Carlo integration. For randomly chosen points inside the simulation box (we selected 1×10^6 points as a sufficient number; however, the convergence occurs usually after a few tens of thousands of iterations), the potential of interactions of Ar with the carbon structure (U_{tot}) at each point was calculated. The criterion determining if a chosen point is inside the carbon structure or in an empty space was $U_{\text{tot}} > U_{sf}$ (0.17 nm) (where 0.17 nm is the assumed carbon atom radius). Tables 2a and 2b show the number of

Table 2a. The number of carbon atoms, volumes and densities of studied carbon structures—initial structure S0 and the same structure with added *fragments 1*.

Structure	Number of carbon atoms in the structure	Volume of carbon structure (nm^3)	d ($g\ cm^{-3}$)
Original structure (S0)	2704	24.7	2.18
S4	2912	26.7	2.18
S8	3120	28.7	2.17
S12	3328	30.5	2.18
S16	3536	32.6	2.16

Table 2b. The number of carbon atoms, volumes and densities of studied carbon structures with added *fragments 2*.

Structure	Number of carbon atoms in the structure	Volume of carbon structure (nm^3)	d ($g\ cm^{-3}$)
S20	3644	33.8	2.15
S24	3752	34.8	2.15
S28	3860	35.8	2.15
S32	3968	37.0	2.14
S35	4049	37.7	2.14

carbon atoms and the densities of ten chosen structures (the data for the remaining structures are collected in the supplementary data available at stacks.iop.org/JPhysCM/19/406208).

2.3. Simulation details—general

For nine generated structures, S0, S4, S8, S16, S20, S24, S28, S32, and S35, Ar adsorption isotherms were simulated. The energy of intermolecular interactions between the atoms x and y (where x and/or y denote Ar (*fluid*) or C (*solid*) atoms) were modelled by the classical Lennard-Jones potential [74]:

$$U_{xy}(r_{xy}) = 4\varepsilon_{xy}\left[\left(\frac{\sigma_{xy}}{r_{xy}}\right)^{12} - \left(\frac{\sigma_{xy}}{r_{xy}}\right)^{6}\right] \tag{1}$$

with the following values of the parameters: $\sigma_{\mathrm{ff}} = 0.34$ nm, and $\varepsilon_{\mathrm{ff}}/k_{\mathrm{B}} = 120.0$ K, $\sigma_{sf} = 0.34$ nm, $\varepsilon_{sf}/k_{\mathrm{B}} = 58.0$ K [75]. The potential cut-off was at $r_{\mathrm{cut},xy} = 5\sigma_{xy}$. The dimensions of the simulation boxes were the same for all structures (4.6 nm × 4.6 nm × 4.6 nm). All isotherms were simulated for a temperature of $T = 87$ K. Periodic boundary conditions were applied in all three directions. The probabilities of a change of the state of the systems via displacement, creation and/or annihilation of the adsorbate atom were the same and were equal to (1/3).

2.4. Simulation details: hyper-parallel tempering Monte Carlo (HPTMC)

We used 43 replicas (i.e. the same number as the number of points on each isotherm). They all have the same temperature but different values of the chemical potential. The number of iterations applied for equilibration was equal to 3×10^6. The histograms were calculated from the next 3×10^6 equilibrium iterations (here one iteration = 30 attempts of the change of the state of each replica in a GCMC way (by displacement, creation or annihilation), and next, one

attempt in the exchange of configurations of atoms in a pair of randomly chosen replicas). The average number of Ar atoms present in each replica was calculated from the histogram by:

$$\langle N \rangle = \sum_{N=0}^{N_{\max}} P(N) \cdot N. \tag{2}$$

2.5. Fitting the simulated isotherms by the DA equation

The DA adsorption isotherm equation was applied in the form:

$$\langle N \rangle_{\mathrm{DA}} = \langle N \rangle_{0\mathrm{DA}} \exp\left[-\left(\frac{A_{\mathrm{pot}}}{\beta E_0} \right)^n \right] \tag{3}$$

where $\langle N \rangle_{\mathrm{DA}}$ and $\langle N \rangle_{0\mathrm{DA}}$ are the number of adsorbed molecules and the adsorption capacity, respectively, β is the affinity parameter (equal to 0.31 for Ar [69]), $A_{\mathrm{pot}} = RT \ln \frac{p_s}{p}$, and p_s is the saturation vapour pressure. E_0 and n (the best fit parameters) are the characteristic energy of adsorption and the parameter of the DA isotherm. Equation (3) was fitted to simulated isotherms in two ranges, i.e. up to 0.1 p/p_s (this range is normally used for experimental data) and in the whole range of relative pressures. Since the fit in the first range for some cases provided too large $\langle N \rangle_{0\mathrm{DA}}$ values, and the fit in the whole range led to satisfactory data, we discuss only the results from the fitting of the whole adsorption isotherm.

The approximation of equation (3) to the simulated data was performed by applying the genetic algorithm (differential evolution (DE)) constructed by Storn and Price [76] and applied successfully by us [77–79]. DE is a very simple heuristic approach for minimizing nonlinear and non-differentiable continuous space functions. To optimize the objective function (ofunc: $(1 - DC)$, where DC is the determination coefficient) with DE, the following settings for the input file are taken into account: the DE/best/2/bin method is chosen (this time, the new vector to be perturbed is the best-performing vector of the current generation); the number of parents (i.e. number of population members), NP, is 10 times greater than the number of parameters of the objective function, D; the weighting factor, F, is equal to 0.8 and the crossover probability constant $CR = 0.5$; the value to reach, VTR, is equal to 10^{-25} (the procedure stops when ofunc $<$ VTR, if either the maximum number of iterations (generations) 'itermax' is reached, or the best parameter vector 'bestmem' has reached a value f(bestmem) $\leqslant$ VTR).

3. Results and discussion

3.1. Porosity and density of studied structures

Figure 2 shows a comparison of the PSDs from the BG method. All structures generated by the MC method are strictly microporous according to the IUPAC system of pore classification [80]. Tables 2a and 2b show the densities of the structures (reported 'true' densities for the series of synthetic 'hard' carbons from polyfurfuryl alcohol are in the range 2.38–2.3 g cm^{-3} [81]). One can see that the addition of structures according to the scheme shown in figure 1 leads to the elimination of porosity in the range 1–2 nm. Consequently, the average pore diameter decreases from 1.25 nm for S0 to 0.61 nm for the structure S35.

3.2. Simulation results

Adsorption isotherms simulated via HPTMC, shown in figures 3 and 4, are snapshots for three selected structures at three relative pressures (movies from supplementary data (available at stacks.iop.org/JPhysCM/19/406208) show the animations of the adsorption process in S0 and S35 structures). From these figures, one can notice that there is full compatibility between

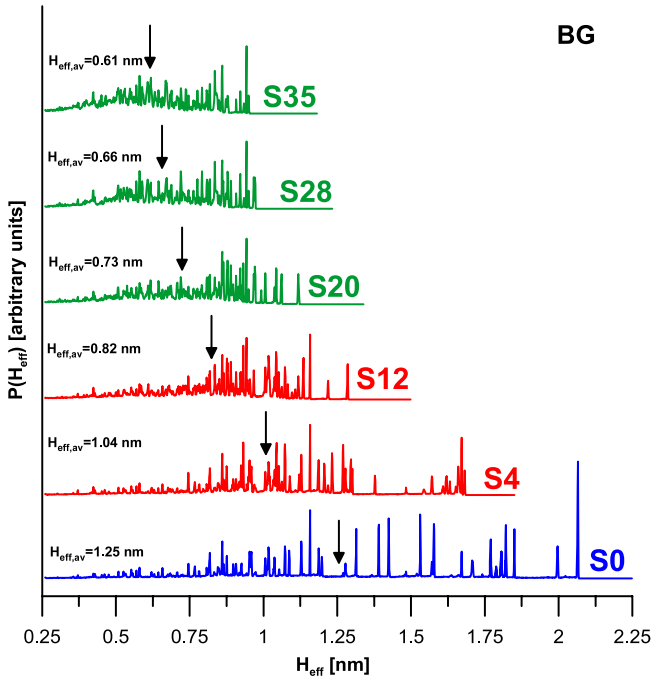

Figure 2. Results of the BG method, showing the evolution of the microporosity of selected structures generated from the MC simulation (following the scheme shown in figure 1). The values of the average effective pore widths ($H_{eff,av}$) are shown by arrows.

the PSD of model structures and the shapes of simulated isotherms. The gradual crowding of the S0 structure (leading finally to S35) by the MC code leads to a decrease in the maximum number of adsorbed molecules, but at low pressures the adsorption progressively increases and the isotherms show the occurrence of more and more homogeneous microporosity in the system. The rising adsorption isotherm and the increasing 'sharpness' of the inflection point with the rise in microporosity and homogeneity of micropore diameters is obvious and was often reported for experimental systems (e.g. [47]).

3.3. Pore size distributions from HK and ND models

Figure 5 shows PSDs calculated from the HK and ND methods. The progressive development of microporosity is seen from the results of both methods; moreover some of the PSDs from ND model show the typical 'gap' at ca. 1 nm. Therefore, the studied models of carbon structures are plausible. The presence of the 'gap' is a consequence of the assumption of a slit-like system of pores in the ND model [14]. The HK method works well since the gap here is absent (as a consequence of the condensation approximation type of approach); however, this method overestimates the microporosity for all structures. Moreover for two models having the widest micropore diameters (S0 and S4) the HK method shows the presence of mesopores. Similar behaviour is observed for the ND method applied for the S0 structure. Generally, correct qualitative behaviour of the ND model is shown in figure 6 where we present the correlation between the average micropore diameters from the ND and BG methods. It can be noticed that the ND model, due to the assumption of slit like porosity, overestimates the pore diameter

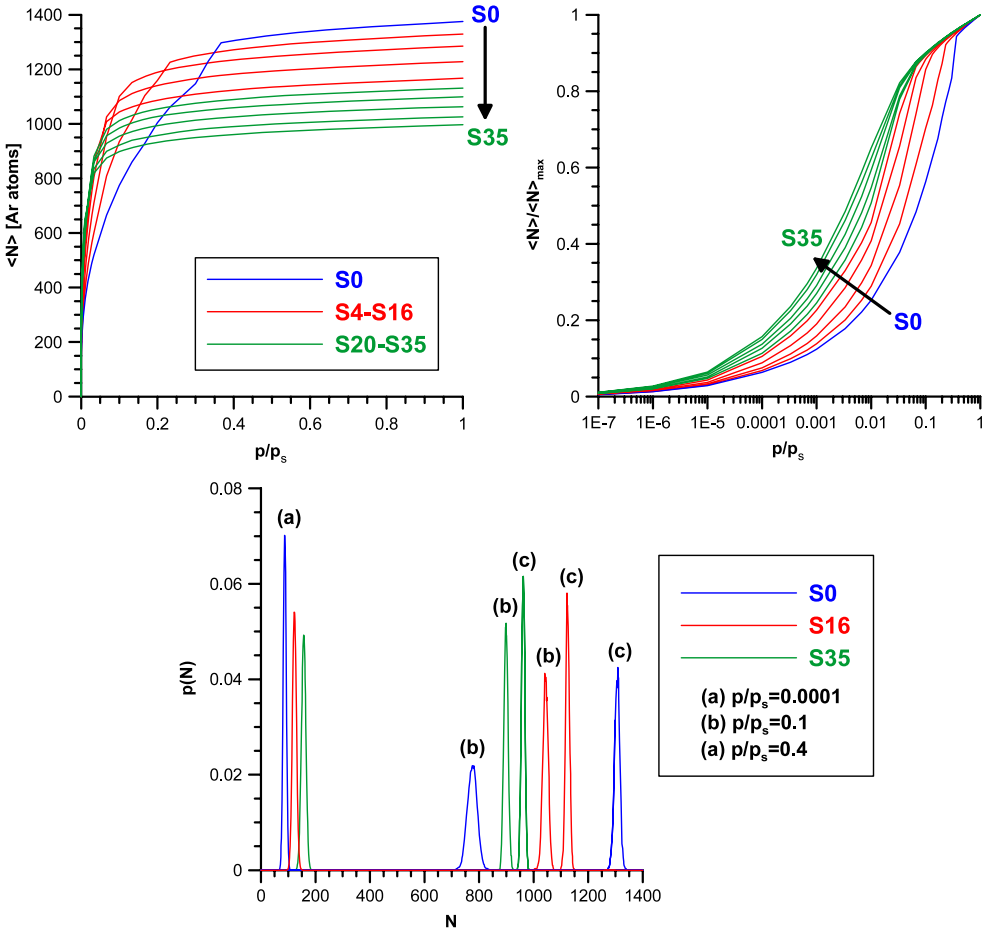

Figure 3. Results of the HPTMC simulation of Ar adsorption (87 K) on studied structures (top figures). The lower figure shows histograms of probability distributions calculated from HPTMC for three selected structures and arbitrarily chosen pressures.

in comparison with the BG method (due to the differences in pore filling pressures mentioned above).

3.4. High-resolution α_s plots and APD curves

The shapes and behaviour of the high-resolution α_s plots and APD curves (figure 7) for simulated data are also very realistic. The plots were obtained by applying, as the reference, Ar adsorption data measured (at 87 K) on non-graphitizing carbon black Cabot BP280, published by Gardner and co-workers [82]. An important common feature of all α_s plots shown in figure 7 is that they start at the point 0.0. This means that the reference system is chosen correctly, and the fullerene-like carbon structures imitate quite well real 'hard' carbons. In comparison with the data simulated for slits, the linear parts of α_s plots are diffused and not so strongly pronounced. Both swings, i.e. FS and CS, are observed on all plots, but the regions where they occur are not so strongly pronounced as for the data simulated for slit-like micropores. This is due to the gradual filling of adsorption space in fullerene-like carbons, and the results obtained

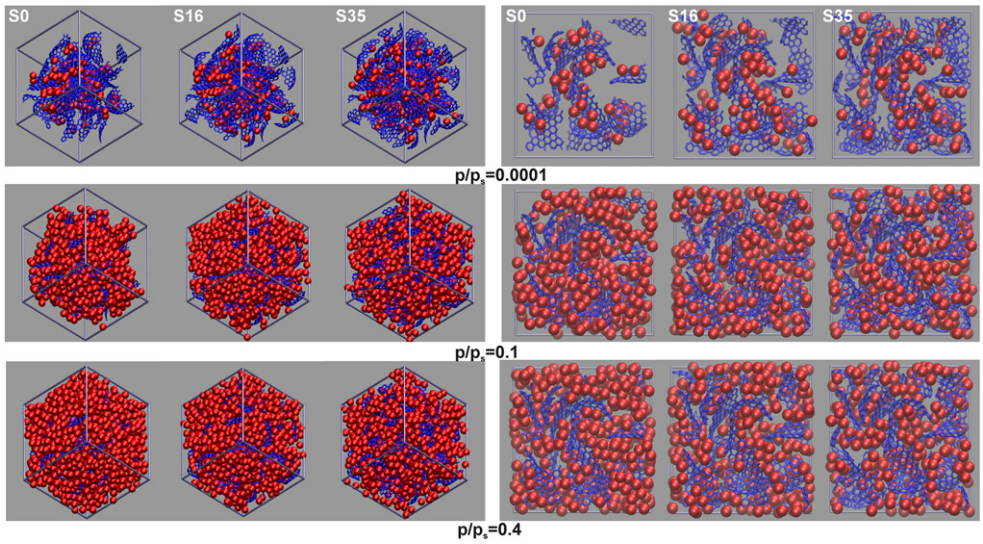

Figure 4. Selected snapshots of equilibrium configurations from HPTMC isotherms generated for S0, S16, and S35 for the following values of the relative pressure, p/p_s: 0.0001, 0.1, and 0.4. Left-hand panels show the whole simulation boxes; right-hand panels show snapshots seen parallel to a surface dividing the boxes into two rectangular prisms.

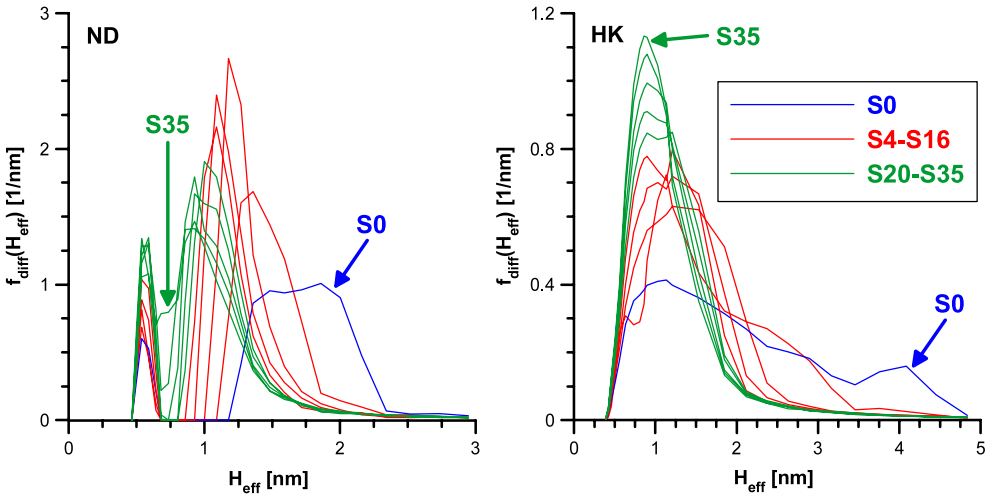

Figure 5. The PSD curves calculated from simulated isotherms using the ND and HK methods.

confirm the conclusions published by Biggs *et al* [46]. For example, the structure S35, having an average pore diameter equal to 0.61 nm, corresponds to the slit-like structure called MS that was studied by Setoyama *et al* [43] (see figure 8 therein). But the corresponding α_s plot shows FS/CS type and not FS type as expected for pores having the slit-like geometry. This is caused by the above-mentioned differences in the filling pressure for the assembly of slit pores, which is lower than for the disordered porous carbon [8].

This can also be confirmed by the analysis of another important empirical correlation recovered from our simulation data (shown in figure 8). An analysis of the APD performed

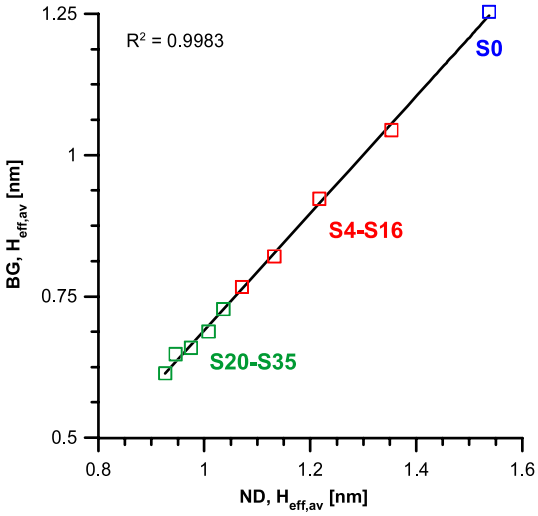

Figure 6. The correlation between the average micropore diameters from BG and ND models.

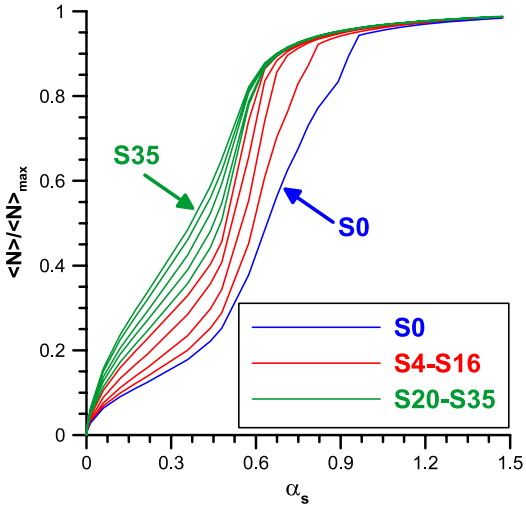

Figure 7. Adsorption isotherms from figure 3, converted into high-resolution α_s plots.

by Kruk *et al* [47] for the series of experimental data measured on synthetic activated carbons showed that two major types of peak can be observed. The first of these (occurring at higher adsorption potential values) is responsible for the monolayer formation (ML) in micropores, whereas the second (recorded in the lower range and called SMF) represents the process of secondary micropore filling. The authors showed that there is an empirical correlation between the maximum value of the adsorption potential and the average micropore diameters calculated from NLDFT for the series of activated carbons (based on low-temperature nitrogen adsorption data). From APD curves calculated for simulated isotherms (shown in figure 8), one can see that, due to strong heterogeneity of our carbon models, overlapping between the ML and SLF peaks usually occurs. However, the relation between the maximum on the APD curve and the pore diameter from the BG method has exactly the same shape as that obtained from

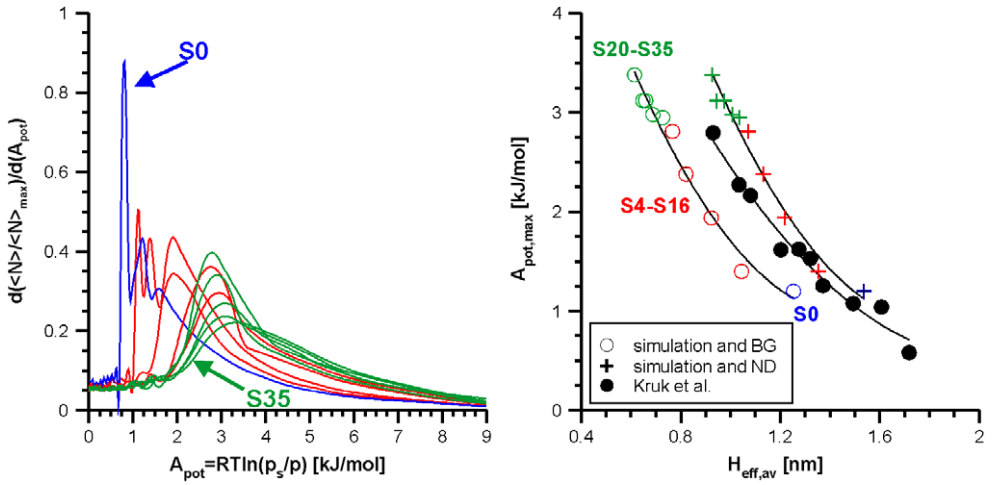

Figure 8. APD curves and the relation between maximum value on the APD for simulated data and average micropore diameters from the BG and ND models. The relation with experimental data published by Kruk *et al* [47] for slit-like micropores is also shown.

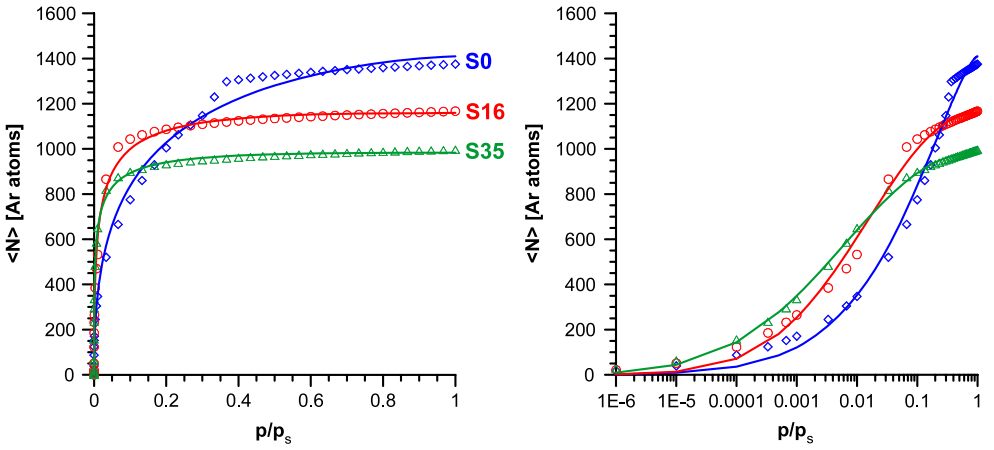

Figure 9. Selected results for the fitting of the DA adsorption isotherm equation (equation (3)) to simulated data.

experimental data by Kruk *et al* (see figure 6 in [47], and figure 8 of this paper). As mentioned above, the maxima on the APD curves confirm that the pore filling pressure is larger in the case of our studied models than in the case of slit-like carbon pores (for example, the value of the adsorption potential of about 2 kJ mol^{-1} is sufficient to fill the pores with slit-like diameters $\sim$1.1 nm, but only with diameters $\sim$0.9 nm for fullerene-like carbon pores).

3.5. The fit of the DA model and the average micropore diameters from different $E_0 = f(H_{\mathrm{eff}})$ relations

Figure 9 shows some examples of fitting the DA model (equation (3)) to simulated data, and table 3 shows the final results. The deviations of the model are observed at very low pressures as a result of neglecting the Henry's law limit in equation (3), and at larger pressures. In the

Table 3. Results of the fitting of simulated data by equation (3) in the whole range of equilibrium pressures.

Ar isotherm for	$\langle N\rangle_{0DA}$	E_0 (kJ mol^{-1})	n	DC
S0	1410	8.522	1.407	0.9945
S4	1340	10.01	1.754	0.9960
S8	1282	11.27	2.055	0.9958
S12	1221	12.35	2.107	0.9966
S16	1159	13.22	2.115	0.9966
S20	1121	13.78	2.130	0.9974
S24	1089	14.34	2.107	0.9982
S28	1052	14.91	2.132	0.9987
S32	1014	15.49	2.128	0.9991
S35	983.4	15.89	2.157	0.9992

latter range the goodness of fit decreases with the rise in pore diameters. Figure 10 shows an important correlation between the maximum number of adsorbed molecules (taken from the plateau on simulated adsorption isotherms) and the $\langle N\rangle_{0DA}$ value calculated from the DA adsorption isotherm equation (equation (3)). The correlation is excellent, and it confirms the validity of equation (3) for describing adsorption data measured for strictly microporous carbons. Moreover, it can be concluded that the DA equation describes adsorption not only in homogeneous systems of pores but also in dispersed ones (as, for example, occurring in the structure S0). Therefore, the assumption about the applicability of equation (3) for describing data only in a homogeneous structure of pores is rather questionable. Further interesting conclusions about the reality of the proposed carbon structures can be drawn from the data shown in figure 10. One can see that the value of E_0 is correlated with the average micropore diameter ($H_{\mathrm{eff,av}}$) calculated from the BG method. This relationship was developed from statistical mechanics by Chen and Yang [72], as mentioned above. These authors proposed the linear relation, and in fact for the studied systems it approaches linearity. On the other hand, the relation between pore diameter and the parameter n of equation (3) is not linear; rather, it can be approximated by at least three straight lines.

Figure 11 is crucial for this part of the study. It summarizes the results of the calculation of the effective pore diameters from the $E_0 = f(H_{\mathrm{eff}})$ relations widely proposed in the literature. To show the similarities in the shapes of the plots, the pore diameters in the first figure were divided by the maximum value generated from each relation for the S0 structure (this value, $H_{\mathrm{eff,av,max}}$, is shown for each relation in the legend). It can be concluded that there are two empirical equations predicting very similar shapes for the plots, as obtained from the simulation results of this study, namely two relationships proposed by Stoeckli. They simply assume a simple inverse relationship between energy and effective micropore diameter. In this figure we also show that the simulated data can be described by:

$$H_{\mathrm{eff}} = \frac{11.7}{E_0} - 0.12. \tag{4}$$

The second figure shows a comparison of absolute values of the average pore diameters. One can see that the previously derived equations overestimate the average pore diameters as a consequence of the differences in pore-filling pressures mentioned above.

4. Conclusions

An MC algorithm proposed in this study for the creation of microporous carbon structures leads to models that imitate very well the adsorption behaviour of experimental 'hard'

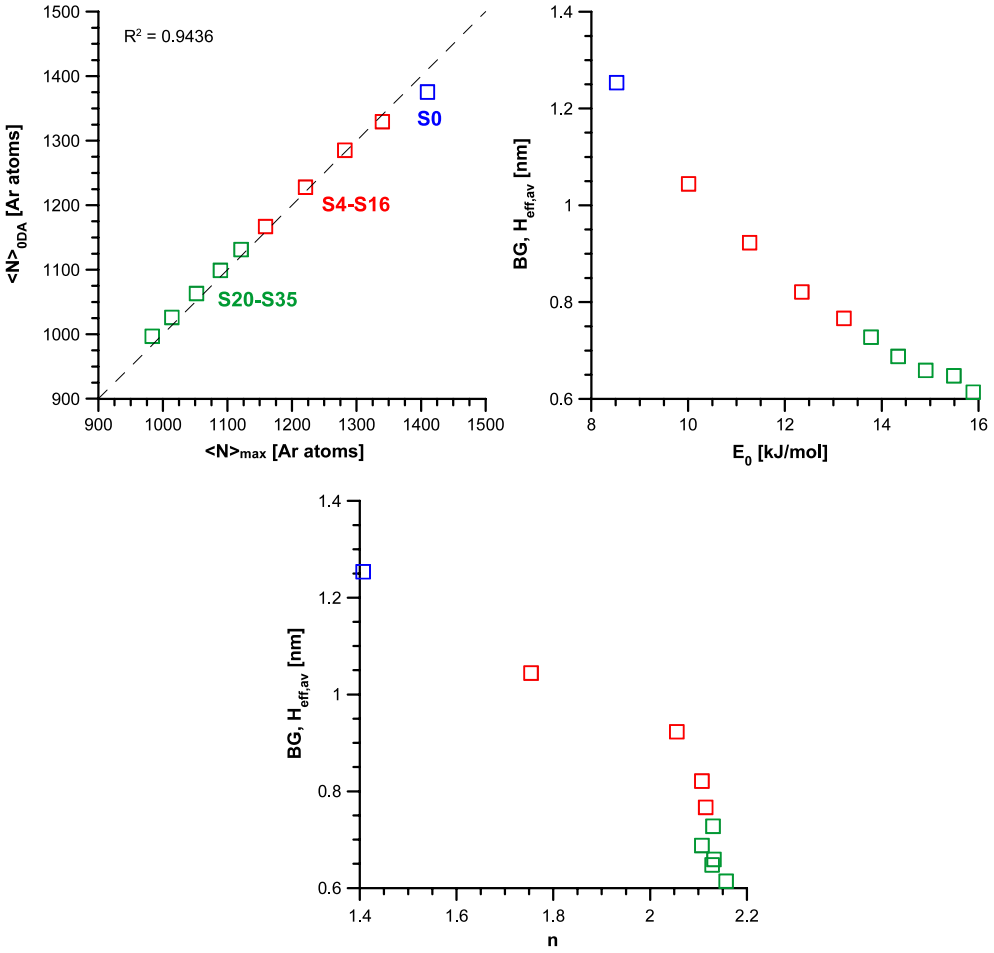

Figure 10. The linear correlation between the $\langle N\rangle_{0\mathrm{DA}}$ (from equation (3) applied to a description of simulated isotherms) and the maximum adsorption from the plateau on adsorption isotherms (a dashed line is plotted for $y = x$), the dependence of the characteristic energy of adsorption E_0 and the parameter n of equation (3) on the average micropore diameters from the BG model.

carbons. The fullerene-like model of microporous carbons is plausible, and leads to shapes and plots of adsorption isotherms fully corresponding to the PSDs calculated from the method (independent of adsorption measurements) proposed by Bhattacharya and Gubbins. Simulated isotherms described by the widely used methods of microporosity characterisation show typical behaviour, as recorded for real adsorbents. The gap in the ND (and NLDFT) PSDs is caused by the assumption of a slit-like geometry of pores, and neglecting pore connectivity. Since the filling pressure for the assembly of slit pores is much lower than that for the disordered porous carbon, the average ND micropore diameters correlate linearly with those from the BG model very well. An empirical relationship between the maximum on the APD curve and the average pore diameter is recovered from simulation data, and confirms the above-mentioned differences in the pore-filling pressures for slits and disordered systems. The DA adsorption isotherm equation correctly predicts the maximum amount of adsorption if the studied system is strictly microporous. Moreover, the simulation data show the validity of the inverse relationship

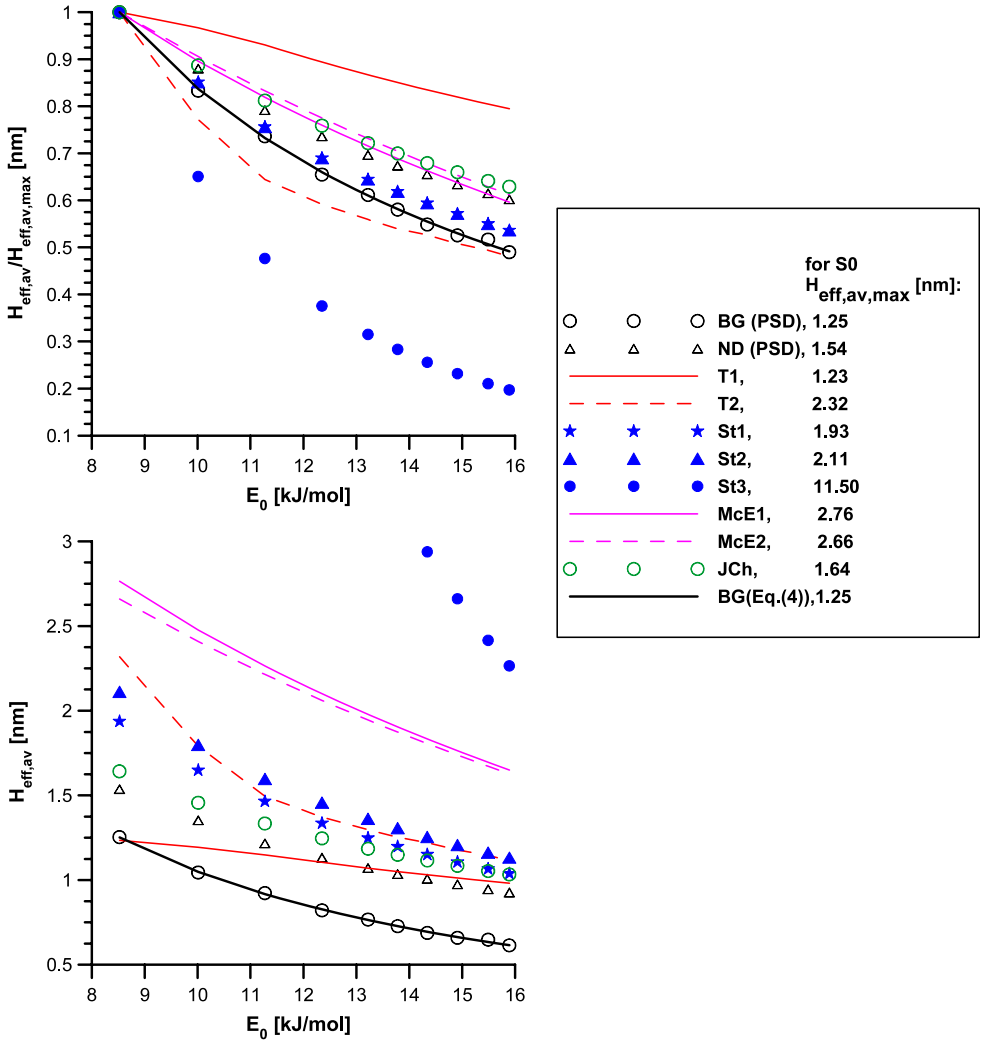

Figure 11. Normalised and absolute micropore diameters calculated from empirical relations given in table 1 (using the parameters from fitting equation (3) for the description of simulated isotherms).

between the characteristic energy of adsorption (E_0) and the average pore diameter. On the other hand, the assumption of the inverse linear relation between the parameter n and the pore diameter is not correct. Simulated Ar adsorption isotherms described by the DA model also confirm the validity of the empirical relationships proposed in the literature between E_0 and H_{eff}. Among them, the two simplest relations proposed by Stoeckli have almost the same shapes as obtained from the simulation data reported in this study.

Acknowledgment

The authors thank professor Stefan Sokołowski (Marii Curie-Skłodowska University, Lublin, Poland) for his help and useful discussions during the preparation of the HPTMC code. We

also acknowledge the use of the computer cluster at Poznań Supercomputing and Networking Center and the Information and Communication Technology Center of the Nicolaus Copernicus University (Toruń, Poland).

References

[1] Bandosz T J, Biggs M J, Gubbins K E, Hattori Y, Iiyama T, Kaneko K, Pikunic J and Thomson K 2003 *Chem. Phys. Carbon* **28** 41
[2] Harris P J F 2003 *Chem. Phys. Carbon* **28** 1
[3] McGreevy R L and Pusztai L 1988 *Mol. Simul.* **1** 359
[4] Thomson K T and Gubbins K E 2000 *Langmuir* **16** 5761
[5] Petersen T, Yarovsky I, Snook I, McCulloch D G and Opleteal G 2003 *Carbon* **41** 2403
[6] Pikunic J, Clinard C, Cohaut N, Gubbins K E, Guet J-M, Pellenq R J-M, Rannou I and Rouzaud J-N 2003 *Langmuir* **19** 8565
[7] Brennan J K, Thomson K T and Gubbins K E 2002 *Langmuir* **18** 5438
[8] Coasne B, Gubbins K E, Hung F R and Jain S K 2006 *Mol. Simul.* **32** 557
[9] Gauden P A, Terzyk A P, Jaroniec M and Kowalczyk P 2007 *J. Colloid Interface Sci.* **310** 205
[10] Ismadji S and Bhatia S K 2001 *Langmuir* **17** 1489
[11] Gauden P A, Kowalczyk P and Terzyk A P 2003 *Langmuir* **19** 4253
[12] Kowalczyk P, Terzyk A P, Gauden P A, Leboda R, Szmechtig-Gauden E, Rychlicki G, Ryu Z and Rong H 2003 *Carbon* **41** 1113
[13] Davies G M and Seaton N A 1998 *Carbon* **36** 1473
[14] Gauden P A, Terzyk A P and Kowalczyk P 2006 *J. Colloid Interface Sci.* **300** 453
[15] Gauden P A, Terzyk A P, Rychlicki G, Kowalczyk P, Ćwiertnia M S and Garbacz J K 2004 *J. Colloid Interface Sci.* **273** 39
[16] Terzyk A P, Furmaniak S, Harris P J F, Gauden P A, Włoch J, Kowalczyk P and Rychlicki G 2007 submitted
[17] Harris P J F and Tsang S C 1997 *Phil. Mag.* A **76** 667
[18] Harris P J F 1997 *Int. Mater. Rev.* **42** 206
[19] Harris P J F, Burian A and Duber S 2000 *Phil. Mag. Lett.* **80** 381
[20] Harris P J F 2005 *Crit. Rev. Solid State Mater Sci.* **30** 235
[21] Acharya M, Strano M S, Mathews J P, Billinge S J L, Petkov V, Subramoneyk S and Foley H C 1999 *Phil. Mag.* B **79** 1499
[22] Smith M A, Foley H C and Lobo R F 2004 *Carbon* **42** 2041
[23] Bourgeois L N and Bursill L A 1999 *Phil. Mag.* A **79** 1155
[24] Goel A, Hebgen P, Vander Sande J B and Howard J B 2002 *Carbon* **40** 177
[25] Goel A, Howard J B and Vander Sande J B 2004 *Carbon* **42** 1907
[26] Grieco W J, Howard J B, Rainey L C and Vander Sande J B 2000 *Carbon* **38** 597
[27] Kumar A, Lobo R F and Wagner N J 2005 *Carbon* **43** 3099
[28] Cataldo F 2002 *Carbon* **40** 157
[29] Bhattacharya S and Gubbins K E 2006 *Langmuir* **22** 7726
[30] Yan Q and de Pablo J 1999 *J. Chem. Phys.* **111** 9509
[31] Horvath G and Kawazoe K 1983 *J. Chem. Eng. Japan* **16** 470
[32] Horvath G 1998 *Colloids Surf.* A **141** 295
[33] Jaroniec M, Choma J and Kruk M 2003 *Colloids Surf.* A **214** 263
[34] Terzyk A P, Gauden P A and Kowalczyk P 2002 *Carbon* **40** 2879
[35] Kowalczyk P, Solarz L, Terzyk AP, Gauden P A and Gun'ko V M 2002 *Shedae Informat.* **MCCLIX** 75
[36] Nguyen C and Do D D 1999 *Langmuir* **15** 3608
[37] Nguyen C and Do D D 2000 *Langmuir* **16** 7218
[38] Do D D, Nguyen C and Do H D 2001 *Colloids Surf.* A **187/188** 51
[39] Do D D and Do H D 2002 *Appl. Surf. Sci.* **78** 1
[40] Do D D and Do H D 2002 *Langmuir* **18** 93
[41] Nguyen C and Do D D 2000 *J. Phys. Chem.* B **104** 11435
[42] Furmaniak S, Terzyk A P, Gauden P A, Lota K, Frąckowiak E, Beguin F and Kowalczyk P 2007 submitted
[43] Setoyama N, Suzuki T and Kaneko K 1998 *Carbon* **36** 1459
[44] Roberts R A, Sing K S W and Tripathi V 1987 *Langmuir* **3** 331
[45] Sing K S W and Rouquerol J 1997 *Handbook of Heterogeneous Catalysis* vol 1, ed G Ertl, H Knözinger and J Weitkamp (Weinheim: VCH) p 427

[46] Biggs M J, Buts A and Williamson D 2004 *Langmuir* **20** 7123
[47] Kruk M, Jaroniec M and Gadkaree K P 1999 *Langmuir* **15** 1442
[48] Dubinin M M 1966 *Chemistry and Physics of Carbon* vol 2, ed P L Walker (New York: Dekker) p 51
[49] Dubinin M M 1975 *Progress in Surface and Membrane Science* vol 9, ed A Cadenhead (New York: Academic) p 1
[50] Dubinin M M 1975 *Adsorption and Porosity* (Warsaw: WAT) (in Polish)
[51] Dubinin M M and Astakhov A V 1971 *Izv. AN SSSR Ser. Khim.* **1** 5 (in Russian)
[52] Dubinin M M and Stoeckli F 1980 *J. Colloid Interface Sci.* **75** 34
[53] Carrott P J M and Ribeiro Carrott M M L 1999 *Carbon* **37** 647
[54] Gauden P A and Terzyk A P 2002 *Theory of Adsorption in Micropores of Carbonaceous Materials* (Warsaw: WICHiR) (in Polish)
[55] Terzyk A P and Gauden P A 2001 *Colloids Surf.* A **177** 57
[56] Terzyk A P, Gauden P A, Zawadzki J, Rychlicki G, Wiśniewski M and Kowalczyk P 2001 *J. Colloid Interface Sci.* **243** 183
[57] Gauden P A 2001 Theoretical description of the structural and energetic heterogeneity of carbonaceous materials *PhD Thesis* (Toruń: UMK) (in Polish)
[58] Terzyk A P, Kowalczyk P, Gauden P A, Rychlicki G and Ziętek S 2002 *Colloids Surf.* A **201** 17
[59] Kowalczyk P, Terzyk A P, Gauden P A and Solarz L 2002 *Comput. Chem.* **26** 125
[60] Kowalczyk P, Terzyk A P, Gauden P A and Rychlicki G 2002 *Adsorpt. Sci. Technol.* **20** 295
[61] Terzyk A P 2003 *J. Colloid Interface Sci.* **268** 301
[62] Terzyk A P, Gauden P A, Rychlicki G and Wojsz R 1998 *Carbon* **36** 1703
Terzyk A P, Gauden P A, Rychlicki G and Wojsz R 1999 *Carbon* **37** 539 (erratum)
[63] Stoeckli H F, Ballerini L and DeBernardini S 1989 *Carbon* **27** 501
[64] Stoeckli H F 1989 *Carbon* **27** 363
[65] Stoeckli H F, Kraehenbuehl F, Ballerini L and DeBernardini S 1989 *Carbon* **27** 125
[66] Stoeckli H F, Rebstein P and Ballerini L 1990 *Carbon* **28** 907
[67] Stoeckli H F, Huguenin D and Laederach A 1994 *Carbon* **32** 1359
[68] Stoeckli H F and Kraehenbuehl F 1986 *Carbon* **22** 297
[69] McEnaney B 1987 *Carbon* **25** 69
[70] McEnaney B and Mays T J 1990 *Proc. COPS II Conf. (Alicante)*
[71] Choma J and Jaroniec M 1997 *Karbo-Energochemia-Ekologia* **11** 368 (in Polish)
[72] Chen S G and Yang R T 1994 *Langmuir* **10** 4244
[73] Humphrey W, Dalke A and Schulten K J 1996 *Mol. Graph.* **14** 33 http://www.ks.uiuc.edu/Research/vmd/
[74] Frenkel D and Smit B 1996 *Understanding Molecular Simulation* (San Diego: Academic)
[75] Miyahara M, Yoshika T and Okazaki M 1997 *J. Chem. Phys.* **106** 8124
[76] Storn R and Price K 1997 *J. Global. Optim.* **11** 341 http://www.icsi.berkeley.edu/~storn/code.html
[77] Furmaniak S, Gauden P A, Terzyk A P, Rychlicki G, Wesołowski R P and Kowalczyk P 2005 *J. Colloid Interf. Sci.* **290** 1
[78] Gauden P A 2005 *J. Colloid Interf. Sci.* **282** 249
[79] Furmaniak S, Terzyk A P, Gauden P A and Rychlicki G 2007 *J. Food Eng.* **79** 718
[80] Sing K S W, Everett D H, Haul R A W, Moscou L, Pierotti R A, Rouquerol J and Siemieniewska T 1985 *Pure Appl. Chem.* **57** 603
[81] Rychlicki G 1985 *The Role of Carbon Chemical Surface Layer Composition in Adsorption and Catalysis* (Toruń: UMK) (in Polish)
[82] Gardner L, Kruk M and Jaroniec M 2001 *J. Phys. Chem.* B **105** 12516